Progress In Electromagnetics Research C, Vol. 20, 173–186, 2011

NOVEL CRLH TL METAMATERIAL AND COMPACT MICROSTRIP BRANCH-LINE COUPLER APPLICATION

H.-X. Xu, G.-M. Wang, and J.-G. Liang

Department of Electromagnetic Field & Microwave Technique
Missile Institute of Air Force Engineering University
Sanyuan 713800, China

Abstract—A novel resonate-type composite right/left handed transmission line (CRLH TL) is presented based on a high-low impedance section and a capacitive gap on the conductor strip, and a Minkowski-loop-shaped complementary split ring resonators (ML-CSRRs) etched on the ground plane. Influence of different iteration orders on the performance of novel CRLH TL and miniaturization mechanism are investigated in depth by electrical simulation (an analysis of circuit model) together with planar electromagnetic (EM) simulation. The close-form results of negative refractive index and complex propagation constant are provided by constitutive parameters retrieval method. For application, a compact branch-line coupler (BLC) centered at 0.88 GHz (GSM band) is designed, fabricated and measured. The upper signal line of CRLH impedance transformer is constructed as Koch curves of first order to facilitate further integration of the BLC. Exact design method for fractal implementation is involved. Measurement results indicate that the proposed coupler achieves a comparable 81% size reduction and good in-band performance with regard to already covered ones. The concept, validated by consistent measurement data, is of practical value for other components design.

1. INTRODUCTION

Branch-line coupler (BLC) [1], which represents a fundamental building block in balanced mixers, modulators and power amplifiers etc., is an important component in planar microwave integrated circuit

Received 18 December 2010, Accepted 28 February 2011, Scheduled 17 March 2011
Corresponding author: He-Xiu Xu (hxxu20008@yahoo.cn).

(MIC). Unfortunately, it suffers a dimension of quarter wavelength, which indicates a large occupied area assuming that the operation band of interest is low. In the case of compactness, several technologies reported in many literatures were utilized to facilitate the integration of the circuit, e.g., BLCs based on composite right/left handed transmission line (CRLH TL) [2–4], adopting fractal geometry [5, 6], using discontinuous microstrip line (ML) [7] and dual transmission line (TL) [8], and even using triple-stub most recently [9]. The non-linear dispersion of CRLH TL allows the dual-band implementation and miniaturization of BLCs to some degree. To be exactly, the hyperbolic dispersion theoretically enables the devices with target phase shifts at any arbitrary two given frequencies and may make the CRLH TL operate at a lower band with the same phase shift relative to conventional TL. However the magnitude of size reduction is far from sufficient for MIC. BLCs reported in [5, 6] have obtained a large size reduction, nevertheless, we should always keep in mind that the adopted higher-order fractal curve (e.g., second order or even higher) also brings another issue of more fabricated complexity as well as worse precision of design process.

The use of a single technology does not always fully fulfill the requirement in terms of compactness. Consequently, the combined technology of fractal geometry and CRLH TL is a good candidate and preferably considered. Recently, the concept of this combined strategy has been recently adopted [10, 11] to develop sub-wavelength particles with a significant lower left handed (LH) band. However, the large insertion loss of CRLH TL in [10] whose peak value is more than 10 dB has limited its popularization in practical application. In view of them, the goal of this article is aimed to propose and synthesize a novel CRLH TL to deal with these drawbacks. The paper is organized as follows. In Section 2, characterization and miniaturization principle of the proposed CRLH TL employing Minkowski-loop-shaped complementary split ring resonators (ML-CSRRs) is researched in depth. Then a simple application of it in the effective design of compact BLC is provided in Section 3. Finally, a major conclusion is highlighted in Section 4.

2. PROPOSED MINIATURIZED CRLH TL

2.1. Configuration and Equivalent Circuit Model

Fractal geometry, specified by iteration factor (IF) and iteration order (IO), is particularly interesting for its strong space-filling property and self-similarity nature. Combining with electromagnetic (EM) theory it has led to an innovative concept and a heated topic in microwave

devices and antennas design. The IF represents the construction law or initiator of the fractal geometry while IO indicates how many iteration processes have been carried out. In this work, Minkowski loop is protuberated in the concentric square CSRRs to form a more compact sub-wavelength CRLH TL. The generation law of Minkowski loop found in [12] is mentioned for completeness and thus is not detailed.

Figure 1 plots the configuration of novel CRLH TL cells and their corresponding lumped-element equivalent T-circuit model. As can be observed, engineered CRLH TL cells are constructed by ML-CSRRs of different IO (realizing negative effective permittivity) etched on the ground plane and capacitive gap (realizing negative effective permeability) on the upper signal strip. Stepped-impedance configuration, introduced on upper conductor strip, is from the point of view of easy impedance match and dealing with the drawback of large insertion loss in [10]. In current design, Minkowski loop is specified by its horizontal IF σ and vertical IF δ. The σ and δ are associated with w_1 and w_2 respectively as follows.

$$w_1 + 2g_4 + g_3 = \sigma(w_3 + 2g_4 + g_3), \tag{1a}$$

$$w_2 = \delta w_3 \tag{1b}$$

Our recent work has shown that the contribution of vertical IF to miniaturization is much more outstanding than that of horizontal IF [13]. As a consequence, the geometrical parameters of ML-CSRRs can be adjusted to benefit large δ for both first- and second-order CSRRs. In this regard, orientation of several fractal bends and physical parameters of second-order CSRRs are changed and different from first-order case. Since fractal perturbation in CSRRs can not result in additional lumped elements in the equivalent T-circuit model, therefore the circuit model of uniform CSRRs-based CRLH TL is also appropriate for ML-CSRRs-based CRLH TL. In this model, ML-CSRRs is described by means of a parallel resonant tank formed by capacitance C_p and inductance L_p, capacitive gap is modeled by means of a capacitance C_g, L_s represents the line inductance, C is composed of the line capacitance and the electric coupling between signal line and ML-CSRRs.

2.2. EM Wave Propagation

To provide a deep insight into the influence of fractal perturbation on performance of CRLH TL, the proposed CRLH particles of different IO are investigated by means of planar EM simulation as well as electrical simulation. During the electrical simulation, we have applied the equivalent T-circuit model in *Ansoft Serenade* to match *S*-parameters of the circuit to the EM simulated ones (characterized

by Ansoft Designer) to extract lumped parameters. Fig. 2 shows the S-parameters of these engineered CRLH TL cells depicted in Fig. 1. As can be observed, frequency responses from EM and electrical simulation are in good agreement which has confirmed the rationality of the model. A further inspection reveals that fundamental LH band has evidently shifted toward lower band as IO increases, which enables an electrically smaller sub-wavelength particle. The shrank effect of frequency seems to be enhanced with increased IO, for instance, the center frequency of the LH band has lowered from 1.09 GHz (zeroth order) to 0.92 GHz (first order), and finally to 0.77 GHz (second order). Thus a maximal frequency reduction of 41.6% is achieved.

Detailed lumped-element parameters of these CRLH TL cells are compared and analyzed in Table 1. It indicates that almost identical

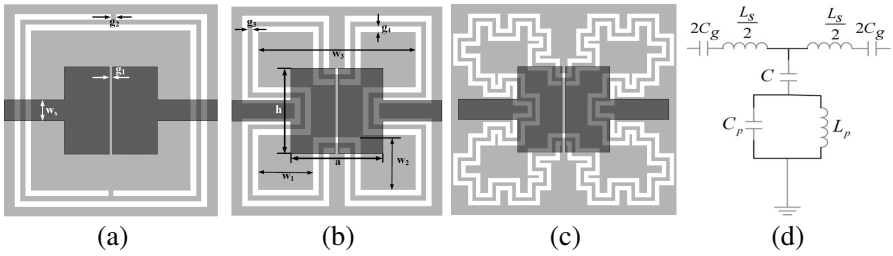

Figure 1. Topology of the proposed CRLH TL cell implemented by ML-CSRRs (depicted in white) of different IO etched on the ground plane (depicted in light grey) and capacitive gap on the upper conductor strip (depicted in dark grey). (a) zeroth order; (b) first order; (c) second order; (d) lumped-element equivalent T-circuit model. The whole dimension of these cells is 16 mm. For zeroth-order ML-CSRRs, $g_2 = g_3 = g_4$=0.4 mm, for first-order case, $g_2 = g_3 = g_4 = 0.4$ mm, σ and δ are set to be 0.39 and 0.31, for second-order case, $g_2 = g_3 = g_4 = 0.3$ mm, σ and δ are set to be 1/3 and 0.25. The residual geometrical parameters are kept identical and listed as: $a = 7$ mm, $h = 6.5$ mm, $w_s = 1.56$ mm, $w_3 = 12$ mm, $g_1 = 0.25$ mm.

Table 1. Extracted lumped parameters of CRLH TL.

ML-CSRRs type	L_s (nH)	C_g (pF)	C (pF)	L_p (nH)	C_p (pF)
Zeroth-order	11.38	0.62	20.1	6.86	0.74
First-order	12.4	058	20	6.31	2.49
Second-order	10.2	0.61	19.9	6.89	3.89

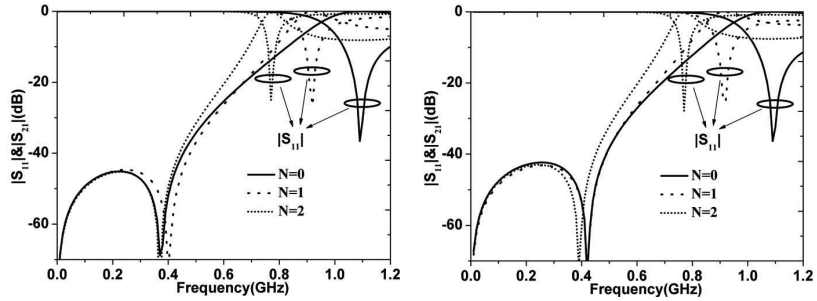

Figure 2. S-parameters of the proposed ML-CSRRs-based CRLH TL cells. (a) EM simulation, (b) electrical simulation. Note that N represents the iteration number.

values of lumped elements except for different capacitance C_p can be concluded. Compared to zeroth-order ML-CSRRs, the value of C_p for second-order ML-CSRRs is more than five times bigger. According to the classical circuit theory, the series resonance frequency f_{se}, shunt resonance frequency f_{sh} (namely the transmission zero), and resonance frequency of the ML-CSRRs f_0 which is the upper limitation of LH band in the vicinity of reflection zero, are determined as follows respectively.

$$f_{se} = \frac{1}{2\pi\sqrt{L_s C_g}}, \tag{2}$$

$$f_{sh} = \frac{1}{2\pi\sqrt{L_p(C_p + C)}}, \tag{3}$$

$$f_0 = \frac{1}{2\pi\sqrt{L_p C_p}}. \tag{4}$$

The f_{se}, associated with the inferior limitation of right handed (RH) band, is less interesting from the point of view of miniaturization. The increased C_p would lead to a reduction of f_{sh} and f_0 referring to Eqs. (3) and (4). However, in practice, f_{sh} is almost unaffected around 0.4 GHz as the value of C_p is too small relative to the coupling capacitance C and contributes less to f_{sh}. From Eq. (4), we conclude that increased C_p is the key factor of resultant decrease of f_0.

Increased C_p mainly attributes to the extension of overall circumference of ML-CSRRs in virtue of space-filling property. It is interesting to mention that, although the total length of ML-CSRRs is in proportion to IO, the inductance L_p haven't increased which is

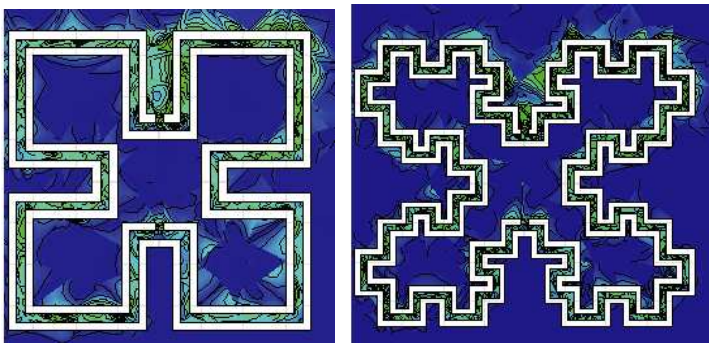

Figure 3. Current distribution of ML-CSRRs in the LH band.

in a completely different mechanism from that of CSRRs using one ring [13]. Almost unaffected L_p is due to the opposite current that happens on the boundary of each ring in some places (inset section) and has inhibited the enhancement of L_p. Fig. 3 depicts the current distribution of ML-CSRRs in the LH band. As can be observed, the current is confined to the fractal boundary of ring slot and is very weak in other places. This phenomenon can not be observed out of the LH band owing to imperfect electric excitation of the gap. The current along the zigzag boundary has significantly extended the current path and results in a larger C_p between metallic places separated by two concentric rings.

To validate the unique LH performance of the CRLH TL including the negative refractive index and backward wave propagation, the proposed particles are studied through constitutive EM parameters retrieval method based on S-parameters.

The effective impedance Z_e and refractive index n are associated with follows after some manipulations from [14]

$$Z_e = \sqrt{\frac{\mu_e}{\varepsilon_e}} = \pm\sqrt{\frac{(1+S_{11})^2 - S_{21}^2}{(1-S_{11})^2 - S_{21}^2}} \tag{5}$$

$$e^{jk_0nd} = \cos(k_0nd) + j\sin(k_0nd) = k \pm \sqrt{k^2-1} \tag{6}$$

n is also related with permittivity and permeability as

$$n = \sqrt{\mu_e\varepsilon_e} \tag{7}$$

whereas ε_e and μ_e are the effective permittivity and permeability respectively. S_{21} and S_{11} are involved with transmission and reflection coefficients respectively, k_0=ω/c is the wave number in the free space, d is the dimension of a CRLH TL cell, and k, without exact physical

meaning, is calculated through

$$k = \left(1 - S_{11}^2 + S_{21}^2\right)/2S_{21} \tag{8}$$

Z_e needs some modification when regard converting the free space propagation to air-filled microstrip line propagation in this work.

$$Z_e = \frac{Z_C}{Z_a} \tag{9}$$

Note Z_c is the characteristic impedance of microstrip line, Z_a is the impedance of air-filled microstrip line which can be determined by the analytical formulae [15]. By solving Eqs. (6) and (8), the expression of real part n can be obtained and is uncertain because of integer m [14]

$$n = \frac{\mathrm{Im}\left[\ln\left(e^{jk_0nd}\right)\right] + 2m\pi - j\mathrm{Re}\left[\ln\left(e^{jk_0nd}\right)\right]}{k_0 d} \tag{10}$$

Here, we apply the method based on Taylor series in [16] which requires mathematical continuous of frequency-dependent ε_e and μ_e to determine the integer m. With fixed Z_e and n, effective permittivity and permeability can be acquired through solving equations provided in (5) and (7), and propagation constant β is achieved by $\beta = k_0 \cdot n$.

Figure 4 shows the retrieved constitutive EM parameters of CRLH TL based on second-order ML-CSRRs. From Fig. 4(a), very obvious negative refractive index and backward wave propagation around 0.77 GHz are obtained. The imaginary part of n, associated with the electric and magnetic losses, almost equals to zero from 0.75 GHz to 0.9 GHz, thus a lossless pass band can be predicted. Further more, the band of non-zero propagation constant is quantitatively identical to that of negative refractive index. From Fig. 4(b), remarkable

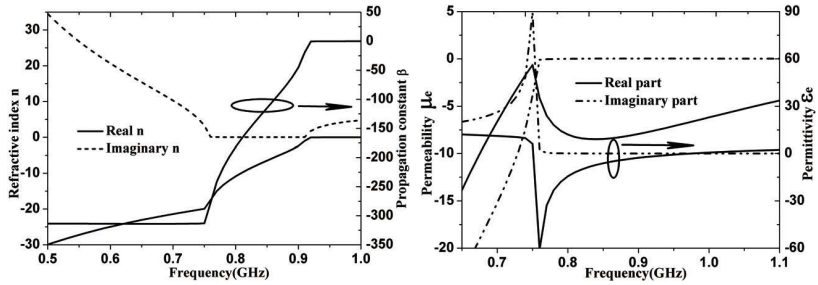

Figure 4. Effective EM parameters retrieved from CRLH TL using second-order ML-CSRRs. (a) Refractive index and propagation constant; (b) effective permittivity and permeability.

electric resonance is obtained around LH band from 0.75 to 0.95 GHz. In the entire frequency band of interest, the effective permeability remains negative. Therefore, the simultaneous negative band is mainly determined by the band of negative permittivity. Fig. 2 gives strong support to the interpretation of all EM phenomena.

3. NOVEL BLC APPLICATION

Conventional BLC is a four-port network consisting of four $\lambda/4$ impedance transformers with phase delay 90°. Note that λ is the guide wavelength at center frequency f_0. Two transformers are with characteristic impedance 50 Ω while the other two 35.3 Ω. In this section, we substitute the ML-CSRRs-based CRLH TL cell with 90° phase advance for conventional $\lambda/4$ transformers to synthesize a compact BLC.

3.1. Design and Theory

The BLC is fabricated on the substrate RT/duroid 5880 with dielectric constant $\varepsilon_r = 2.2$, thickness $h = 0.508$ mm. Second-order ML-CSRRs may lead to a large insertion loss due to the radiation loss of engineered fractal-shaped defected ground structure. As a consequence, the applied first-order ML-CSRRs is a trade-off between the miniaturization and the performance of BLC. Let us first begin with the fundamental Bloch-Floquet theory in the analysis and synthesis of 35.5 Ω and 50 Ω CRLH impedance transformers. The phase shift per cell φ and Bloch impedance Z_β, which are the key parameters for microwave circuit design, are given as

$$\cos\varphi = \cos(\beta d) = 1 + \frac{Z_s(j\omega)}{Z_p(j\omega)}, \tag{11}$$

$$Z_\beta = \sqrt{Z_s(j\omega)[Z_s(j\omega) + 2Z_p(j\omega)]}. \tag{12}$$

where $Z_s(j\omega)$ is the impedance of series branch, $Z_p(j\omega)$ is the impedance of shunt branch. The lower and upper limitation of the LH band is determined by two frequencies f_L and f_0. The calculation of f_L is achieved just by driving Z_β to zero. At f_L and f_0, both φ and Z_β take extreme values which theoretically enables us to implement $\lambda/4$ impedance transformers with controllable positive phase and impedance across a wide range. In current design, Z_β is set to be 35.5 Ω and 50 Ω while φ is set to be +90° for both transformers at target frequency 0.88 GHz respectively.

The main design procedure involves four steps. First, apply the circuit model in *Ansoft Serenade* to synthesize a $\lambda/4$ impedance

Table 2. Geometrical Parameters of CRLH impedance transformer (unit: mm).

Transformer type	w_s	h	a	w_1	w_2	w_3	g_1	g_2	g_3	g_4	L
35.3 Ω	2.5	6.5	6	4	4.2	12	0.25	0.4	0.4	0.4	49
50 Ω	1.6	6.5	7	4	4.2	12	0.25	0.4	0.4	0.4	38

transformer with specified electrical performance. There should be many groups of solutions which can fulfill the circuit model, however, some solutions may fail and must be ruled out. As a consequence, the next step lies in insetting the achieved lumped-element parameters into expressions Eqs. (11) and (12) to select the correct solution. Third, with decided lumped elements, the geometrical parameters of the physical structure can be synthesized, e.g., the length L and width w_s of microstrip line are adjusted according to L_s and Z_C, the width and height of capacitive gap are determined corresponding to C_g through analytical equations in [17], the dimensions of ML-CSRRs, which mainly determines the frequency f_0, are optimized according to L_p, C_p, and finally the width of low impedance section is tuned according to C. With fixed physical parameters of 35.5 Ω and 50 Ω $\lambda/4$ impedance transformer (shown in Table 2), the last step is considered constructing upper signal line as Koch curves of first order for further size reduction.

As to fractal implementation, fractal right-angle bends replaced by chamfered bends is from the point of decreasing current discontinuity. It is useful to mention that chamfered bend can not avoid but can minimize the discontinuity. As the key factor of transmission phase shift, the reactance induced by non-negligible discontinuity must be properly evaluated if one wants to exactly design fractal-shaped microstrip line with a specified phase. The length L of conventional line must be reduced by Δd per bend to compensate for fractal-shaped line, where Δd is given by [18]

$$\Delta d = \frac{19.2\pi h}{\sqrt{\varepsilon_{eff}} Z_C} \left[2 - \left(f_0 h / 0.4 Z_C \right)^2 \right] \tag{13}$$

In Eq. (12), ε_{eff} is the effective dielectric constant, and h is the height of substrate in mm. From the formula given above, L can be roughly engineered. Note that the final optimization around L is very essential for exact design. Fig. 5 displays the EM simulated S-parameters of 35.3 Ω and 50 Ω fractal-shaped impedance transformers respectively. It reveals that both transformers operating at 0.88 GHz

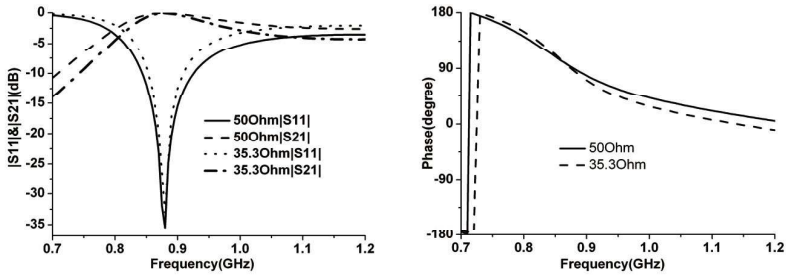

(a) (b)

Figure 5. S-parameters of 35.3 and 50 Ω impedance transformer. (a) Return and insertion loss; (b) transmission phase response.

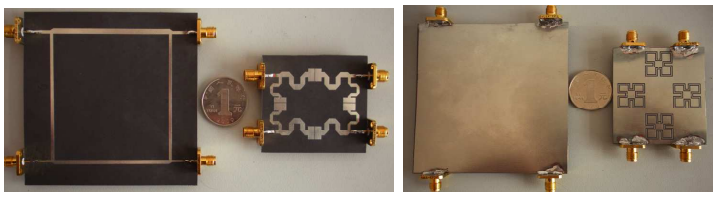

(a) (b)

Figure 6. Fabricated prototypes of conventional and proposed BLCs. (a) Top view; (b) bottom view.

obtain 90° phase advance from the nonlinear transmission phase response. Further more, the impedance match of port 1 whose return loss better than 35 dB is very comparable. Exact results of both transformers have demonstrated the rationality of the design.

3.2. Illustrative Results

By assembling the designed fractal-shaped 35.5 Ω and 50 Ω impedance transformers, a compact BLC is developed. To experimentally validate the effectiveness of combined technology in BLC design, an example coupler is fabricated and measured. Conventional BLC is also designed and fabricated for comparison convenience. Fig. 6 shows the fabricated prototypes of conventional and novel designed BLCs. As can be seen, the footprint which the proposed coupler occupies ($34 \times 25\,\text{mm}^2$) is significantly reduced by approximate 80% relative to its conventional counterpart ($63.5 \times 66.5\,\text{mm}^2$). Thus a higher level of miniaturization factor is obtained compared to the first-order BLC (64.6%) reported in [5].

Figure 7 exhibits the simulated (characterized by Ansoft Designer)

and measured (characterized by Anritsu ME7808A vector network analyzer) S-parameters of the proposed BLC. Fig. 8 plots the simulated and measured transmission phase imbalance between port 2 and 3. Reasonable agreement between simulation and measurement can be observed in the whole frequency band of interest except for slight frequency shift toward lower band 0.87 GHz for measurement case. This slight discrepancy is partly attributing to the tolerances that are inherent in the fabrication process. However, the most significant factor is the small fractal dimensions of ML-CSRRs. The precision is influenced by the size of the mesh grids when using the MoM-based *Ansoft Designer* to analyze complicated structures. Thus the simulation results of the designed coupler may be with low precision.

Detailed measurement performance of the proposed BLC and its conventional counterpart are compared and summarized in Table 3.

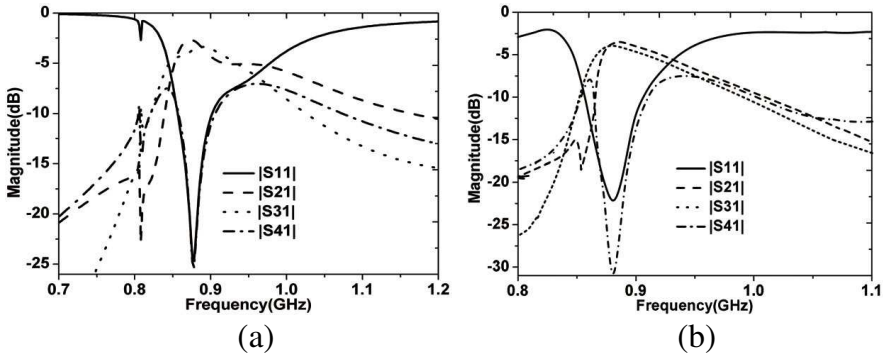

Figure 7. S-parameters of developed BLC. (a) Simulation, (b) measurement.

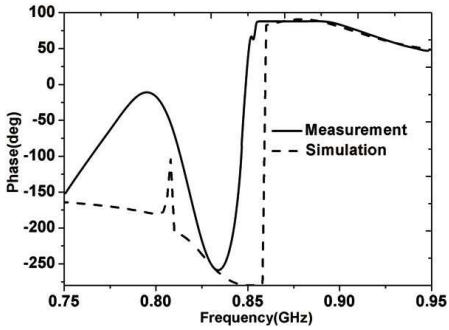

Figure 8. Transmission phase imbalance $|\angle S_{21} - \angle S_{31}|$ between port 2 and 3.

Table 3. Comparison of measurement results of conventional and novel designed BLC.

BLC type	CF	RIL	IL	PI	BW_1	BW_2
Conventional	0.88	29.92, 28.1	3.5, 3.6	90.7	25.1	20.6
Novel design	0.87	22.3, 31.4	3.6, 4.1	90.3	9.6	6.5

Note: CF represents center frequency f_0 in GHz, RIL means the return and isolation loss $|S_{11}|$ & $|S_{41}|$ at f_0 in dB, IL represents insertion loss $|S_{21}|$ & $|S_{31}|$ at f_0 in dB, PI means the phase imbalance $\angle S_{31} - \angle S_{21}$ between port 2 and 3 in deg, BW_1 means communal relative bandwidth of 10 dB return and isolation loss $(f_2 - f_1)/f_0$ in %, BW_2 means relative bandwidth of phase imbalance $(||\angle S_{21} - \angle S_{31}| - 90°| \leq 3^0)$ in %.

Table 4. Comparison of compact BLCs.

BLCs	[2]	[4]	[5]	[6]	[7]	[8]	[9]	**Proposed**
Scale of miniaturization	39.2%	10%	81.8% 64.6%	75.3%	60%	63.9%	44%	**81%**

The narrower bandwidth of the proposed BLC can be successfully interpreted through the relatively steep phase response of impedance transformer (depicted in Fig. 5). It also indicates that the proposed coupler has larger insertion loss, which should be explained by several utilized bends and ML-CSRRs. Our laboratorial work shows that the greater number of ML-CSRRs and bends is, the larger insertion loss becomes. Nevertheless, insertion loss of the proposed BLC (3.6 and 4.1 dB) is within the scope of normal level in practice and very comparable with regard to already covered BLCs, e.g., 4.19 and 4.31 dB for the lower band while 4.43 and 4.72 dB for the upper band [2], almost 4 and 5 dB for the second-order BLC [5]. The exact phase imbalance with 90.3° should be highlighted when compared to 93° [2] and 86.8° [3]. What's more, the proposed BLC is with easier design procedure relative to ones covered in [9] (many stubs) and [7] (many capacitive and inductive lines).

Since the measured f_0 shifts toward lower band, the proposed BLC achieves a further 81% size reduction. Comparison of miniaturization performance of the BLCs between this paper and previous works is highlighted in Table 4. To the author's best knowledge, the designed BLC even achieves one of the largest miniaturization among the available data.

4. CONCLUSION

It has been successfully proved that the combined technology of CRLH TL and fractal geometry results in a significant size reduction and demonstrated without any significant performance deterioration of the BLC. Advantages of the technique in current design may be highlighted as follows: (1) compact in size, (2) good passband performance (3) easy fabrication without any via and lumped elements. Disadvantage mainly lies in relative narrow bandwidth. However, it can be solved by tuning physical parameters of CSRRs to make the phase response less sensitive. Nevertheless, the combined technology provides us an alternative approach and an innovative concept in microwave devices design.

ACKNOWLEDGMENT

This work is supported by the National Natural Science Foundation of China under Grant No. 60971118. Special thanks should also be delivered to the China North Electronic Engineering Research Institute for the fabrication.

REFERENCES

1. Pozar, D. M., *Microwave Engineering*, 3rd edition, Wiley, New York, 2005.
2. Bonache, J., G. Sisó, M. Gil, et al., "Application of composite right/left handed (CRLH) transmission lines based on complementary split ring resonators (CSRRs) to the design of dual-band microwave components," *IEEE Microw. Wireless Compon. Lett.*, Vol. 18, No. 8, 524–526, 2008.
3. Zhang, Y., L. Hu, and S.-L. He, "A tunable dual-broadband branch-line coupler utilizing composite right/left-handed transmission lines," *Journal of Zhejiang University Science*, Vol. 6A, No. 6, 483–486, 2005.
4. Chi, P.-L. and T. Itoh, "Miniaturized dual-band directional couplers using composite right/left-handed transmission structures and their applications," *IEEE Trans. Microw. Theory Tech.*, Vol. 57, No. 5, 1207–1215, 2009.
5. Chen, W.-L. and G.-M. Wang, "Design of novel miniaturized fractal-shaped branch-line couplers," *Microwave Opt. Technol. Lett.*, Vol. 50, No. 5, 1198–1201, 2008.

6. Ghali, H. and T. A. Moselhy, "Miniaturized fractal rat-race,branch-line and coupled-line hybrids," *IEEE Trans. Microw. Theory Tech.*, Vol. 52, No. 11, 2513–2520, 2004.
7. Sun, K.-O., S.-J. Ho, C.-C. Yen, and D. van der Weide, "A compact branch-line coupler using discontinuous microstrip lines," *IEEE Microw. Wireless Compon. Lett.*, Vol. 15, No. 8, 519–520, 2005.
8. Tang, C.-W., M.-G. Chen, and C.-H. Tsai, "Miniaturization of microstrip branch-line coupler with dual transmission lines," *IEEE Microw. Wireless Compon. Lett.*, Vol. 18, No. 3, 185–187, 2008.
9. Li, B., X. Wu, and W. Wu, "A Miniaturized branch-line coupler with wideband harmonics suppression," *Progress In Electromagnetics Research Letters*, Vol. 17, 181–189, 2010.
10. Crnojević-Bengin, V., V. Radonić, and B. Jokanović, "Fractal geometries of complementary split-ring resonators," *IEEE Trans. Microw. Theory Tech.*, Vol. 56, No. 10, 2312–2321, 2008.
11. Xu, H.-X., G.-M. Wang, C.-X. Zhang, and Y. Hu, "Microstrip approach benefits quad splitter," Microwaves & RF, Vol. 49, No. 6, 92–96, 2010.
12. Falconer, K., *Fractal Geometry*, J. Wiley & Sons, New York, 2003.
13. Xu, H.-X., G.-M. Wang, C.-X. Zhang, and K. Lu, "Novel design of composite right/left handed transmission line based on fractal shaped geometry of complementary split ring resonators," *Journal of Engineering Design*, Vol. 18, No. 1, 71–76, 2011.
14. Smith, D. R., S. Schultz, P. Markos, and C. M. Soukoulis, "Determination of effective permittivity and permeability of metamaterials from reflection and transmission coefficients," *Phys. Rev. B*, Vol. 65, 195104, 2002.
15. Itoh, T., *Planar Transmission Line Structures*, IEEE Press, New York, 1987.
16. Chen, X., T. M. Grzegorczyk, B.-I. Wu, et al., "Robust method to retrieve the constitutive effective parameters of metamaterials," *Phys. Rev. E*, Vol. 70, 016608, 2004.
17. Wang, W.-X., *Microwave Engineering*, Ch. 5, 128–129, China National Defense Industry Press, Beijing, 2009.
18. Bahl, I., *Lumped Elements for RF and Microwave Circuits*, Ch. 14, 462–465, Artech House, Boston, 2003.